Proceedings of ASME Turbo Expo 2011
GT2011
June 6-10, 2011, Vancouver, British Columbia, Canada

GT2011-45927

INFLUENCE OF SHOCK WAVE ON TURBINE VANE SUCTION SIDE FILM COOLING WITH COMPOUND-ANGLE SHAPED HOLES

K. Liu, D. P. Narzary, and J. C. Han
Turbine Heat Transfer Laboratory
Department of Mechanical Engineering
Texas A&M University
College Station, TX 77843-3123
Email: jc-han@tamu.edu

A. V. Mirzamoghadam and A. Riahi
Honeywell International
Turbine Department
111 S. 34th Street
Phoenix, AZ 85034

ABSTRACT

This paper studies the effect of shock wave on turbine vane suction side film cooling using a conduction-free Pressure Sensitive Paint (PSP) technique. Tests were performed in a five-vane annular cascade with a blow-down flow loop facility. The exit Mach numbers are controlled to be 0.7, 1.1, and 1.3, from subsonic to transonic flow conditions. Two foreign gases N_2 and CO_2 are selected to study the effects of two coolant-to-mainstream density ratios, 1.0 and 1.5, on film cooling. Four averaged coolant blowing ratios in the range, 0.4 to 1.6 are investigated. The test vane features 3 rows of radial-angle cylindrical holes around the leading edge, and 2 rows of compound-angle shaped holes on the suction side. Results suggest that the PSP is an accurate technique capable of producing clear and detailed film cooling effectiveness contours at transonic flow conditions. At lower blowing ratio, film cooling effectiveness decreases with increasing exit Mach number. On the other hand, an opposite trend is observed at high blowing ratio. In transonic flow, the rapid rise in pressure caused by shock benefits film-cooling by deflecting the coolant jet toward the vane surface at higher blowing ratio. Results show that denser coolant performs better, typically at higher blowing ratio in transonic flow. Results also show that the optimum momentum flux ratio decreases with density ratio at subsonic condition. In transonic flow, however, the trend is reversed and the peak effectiveness values plateau over a long range of momentum flux ratio.

NOMENCLATURE

Cx	axial chord length of the stator vane, *in*
d	diameter of film cooling hole, *in*
DR	density ratio = ρ_c/ρ_m
H	vane height, *in*
I	image pixel intensity, momentum flux ratio
L	actual vane surface length, *in*
LE	leading edge of vane
M	blowing ratio = $(\rho V)_c/(\rho V)_m$
Ma	Mach number
P	partial pressure, *psi*
s	hole-to-hole spacing, equivalent slot width, *in*
TE	trailing edge of vane
V	velocity, *ft/s*
W	molecular weight, *lbm/lbmol*
X	surface distance from vane leading edge, *in*
y	spanwise distance from hub, *in*
η	film cooling effectiveness
ρ	fluid density, *lbm/ft*^{3}

Subscript

blk	black image
c	coolant
exit	exit condition
fg	foreign gas
m	mainstream
mix	mainstream air coolant mixture
ref	reference image

INTRODUCTION

The initial stages of the turbine are constantly exposed to high temperatures from gases exiting the combustion chamber. In pursuit of higher thermal efficiencies, gas turbines are operated at first stage inlet temperatures around 1500°C resulting in excessive thermal stresses on the turbine components. Continuous operation under high turbine inlet temperatures enhances the possibility of thermal failure of the hot gas path components. The life of the turbine airfoils can be

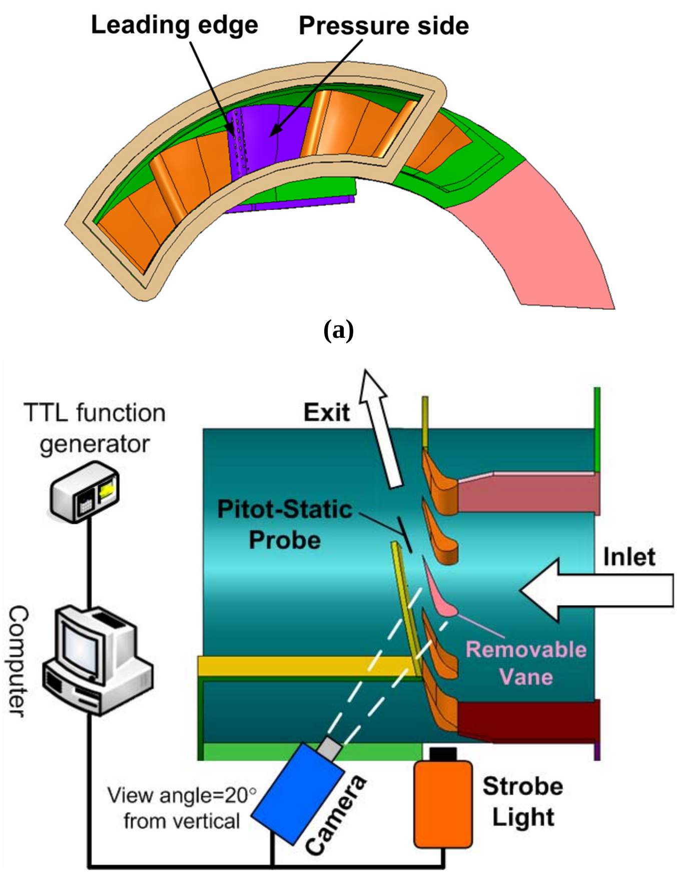

(a)

(b)

Fig. 1 (a) Annular 5-vane cascade (b) Schematic of optical setup

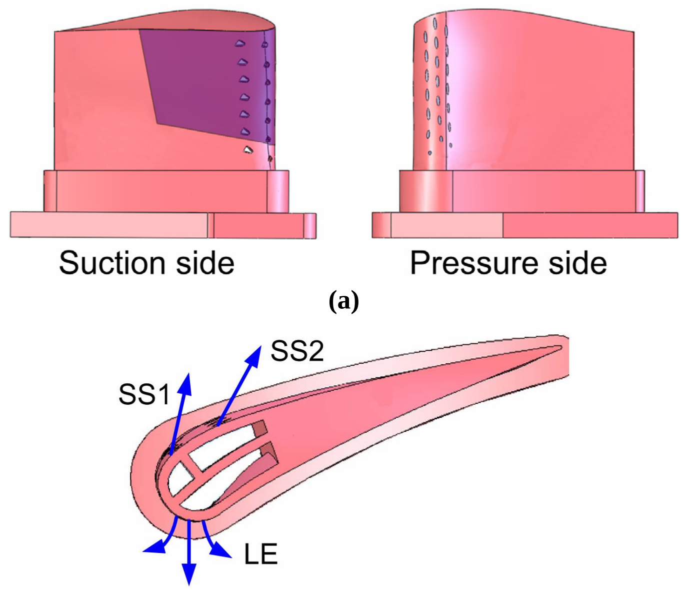

(a)

(b)

Fig. 2 Test Vane (a) hole locations (b) coolant passage locations [Shaded area: data taken region]

increased by implementing any of a variety of cooling techniques encapsulated by Han et al. [1]. Film cooling is an external cooling technique commonly used in conjunction with internal cooling to protect the turbine components from the mainstream hot gas. In film cooling, the ejected coolant displaces the mainstream boundary layer creating a protective film on the surface of the exposed component. The location of the coolant holes, their geometry and the quantity of the coolant gases are critical in providing proper coolant film protection.

The subject of film cooling has been extensively studied over the last decades, thorough reviews of the parameters affecting film cooling are provided by Goldstein [2], Han et al. [1], Bunker [3], Bogard and Thole [4], and Han and Rallabandi [5].

Ligrani et al. [6] reported that injecting the film coolant at an angle to the mainstream results in higher film cooling effectiveness, due to greater lateral diffusion of the coolant. Schmidt et al. [7] demonstrated that compound-angled holes provide better coolant coverage than straight holes. They observed that 60^{o} compound angled holes, with and without forward expanded shaped exit, have significantly greater effectiveness than cylindrical holes aligned with the mainstream at larger momentum flux ratios. Several studies in the open literature (Ekkad et al. [8], Wright et al. [9], and Goldstein and Jin [10]) arrived at similar conclusions using different experimental techniques. Ito et al. [11] showed the effect of curvature on film cooling effectiveness, they reported higher effectiveness on a convex surface than on a flat plate at low momentum flux ratio and the reverse at high momentum flux ratio. The trend is reversed on concave wall.

Sinha et al. [12] observed a significant improvement in film cooling effectiveness at higher density ratios due to the suppression of lift-off. They found good scaling of film cooling effectiveness with blowing ratio for lower blowing conditions, however, momentum flux ratio was more relevant at higher blowing conditions. Ethridge [13] et al. conducted tests on the suction side of a first-stage turbine vane with density ratio ranges from 1.1 to 1.6 and blowing ratio ranging drew from 0.2 to 1.5, and draw similar conclusions. Typical coolant to mainstream density ratios in gas turbine engines range between 2.0 to 3.0. To simulate the actual engine conditions, foreign gases have been used to study the effect of density ratio. Goldstein [14] demonstrated that film cooling performance with higher density ratio has significantly improvement on the surface downstream of the ejection location, particularly at high blowing ratios.

Recently, transonic film cooling has been studied in the literature. Ligrani et al [15] used flat plate to investigate the interaction between shock waves and film cooling. The test parameters were - mainstream Mach numbers of 0.8 and 1.1-1.12, with density ratio of 1.5-1.6. A row of three cylindrical holes with 30° inclined angle are used in the study. They reported the effectiveness is generally higher when shock waves are present when a plenum condition was used. Several

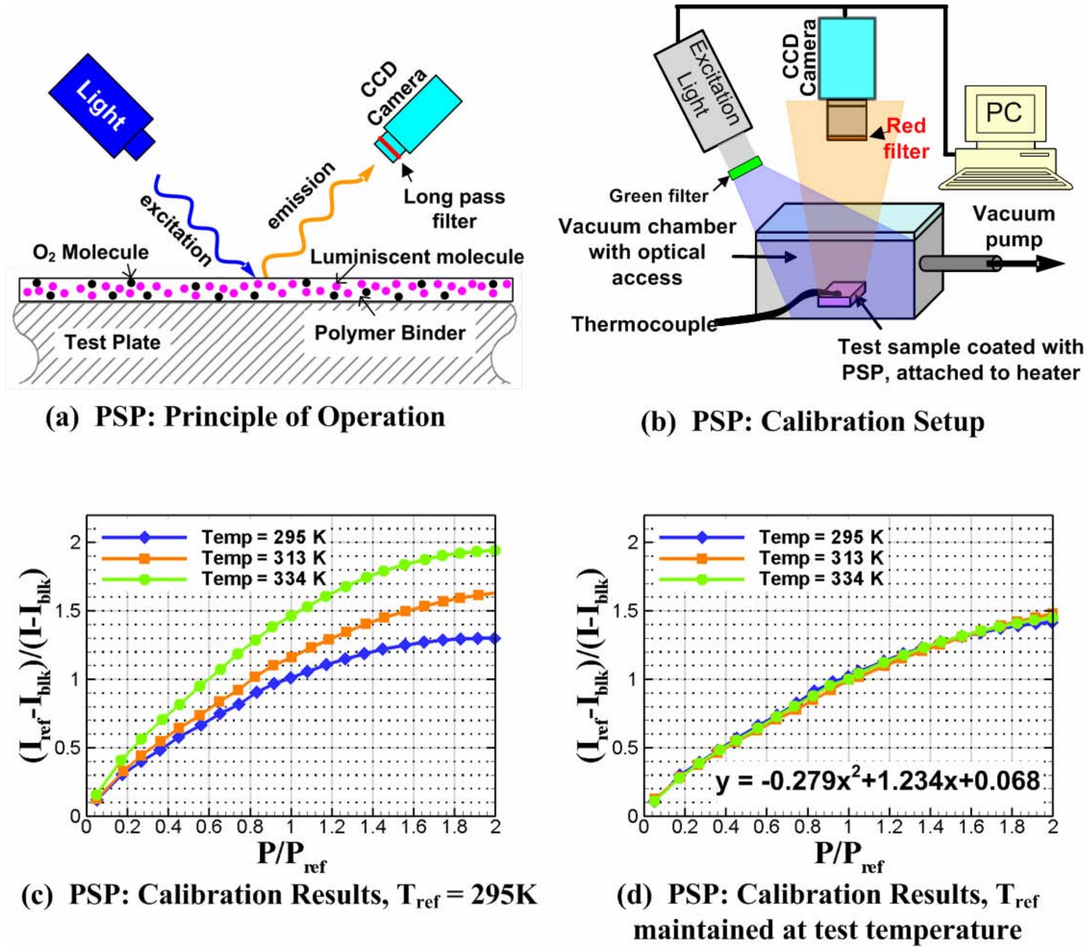

Fig. 3 PSP working principle, calibration

studies examined various parametric effects on film cooling on transonic airfoil by other groups. Furukawa and Ligrani [16] used symmetric airfoil model to study film effectiveness from different geometry of film cooling hole and concluded the compound-angle shaped holes perform better than axial shaped holes and axial cylindrical holes. Kodzwa and Eaton [17] demonstrated that the increasing coolant density ratio improves effectiveness when the coolant jets are attached to the surface. Flow field measurements are carried out by using Schlieren pictures to visualize shocks, wakes, and separation zones. Flow patterns of transonic airfoil (Sonoda et al. [18]) and transonic turbine stage (de la Loma et al. [19]), show that the complex shock originated at the vane trailing edge and reflected in two directions, one to the downstream rotor, and the other one to the neighboring vane which impinges on the suction side vane throat region.

The Turbine Heat Transfer Laboratory (THTL) at Texas A&M University has undertaken a series of studies on film-cooling in their 5-blade linear cascade facility. Mhetras and Han [20], Narzary et al. [21], and Gao et al. [22] studied film-cooling in blades featuring compound cylindrical holes, compound shaped holes, and axial shaped holes, respectively. Between the three blades, compound shaped holes produced the highest effectiveness on the suction side followed by compound cylindrical holes and axial shaped holes at a given blowing ratio.

Several experimental techniques have been used in the literature to determine film cooling effectiveness. For almost identical conditions, the thermal methods result in a higher film cooling effectiveness than corresponding mass transfer analogy due to lateral conduction in the low conductivity substrate plate in regions of high thermal gradients. This issue has been discussed by Nicoll and Whitelaw [23], Wright et al. [9], and Goldstein and Jin [10]. The present study attempts at investigating the effects of shock wave, coolant density and blowing ratio over the suction side. Results are presented in the form of effectiveness contours and spanwise-averaged plots. Pressure Sensitive Paint (PSP) technique is used to obtain the effectiveness. Being a mass transfer technique, it is free from heat conduction related errors frequently encountered in other film-cooling measurement techniques such as Transient Liquid Crystal (TLC), Infrared (IR), and Temperature Sensitive Paint (TSP). The measurement is non-intrusive in nature and renders high resolution images, making it one of the most powerful techniques available today.

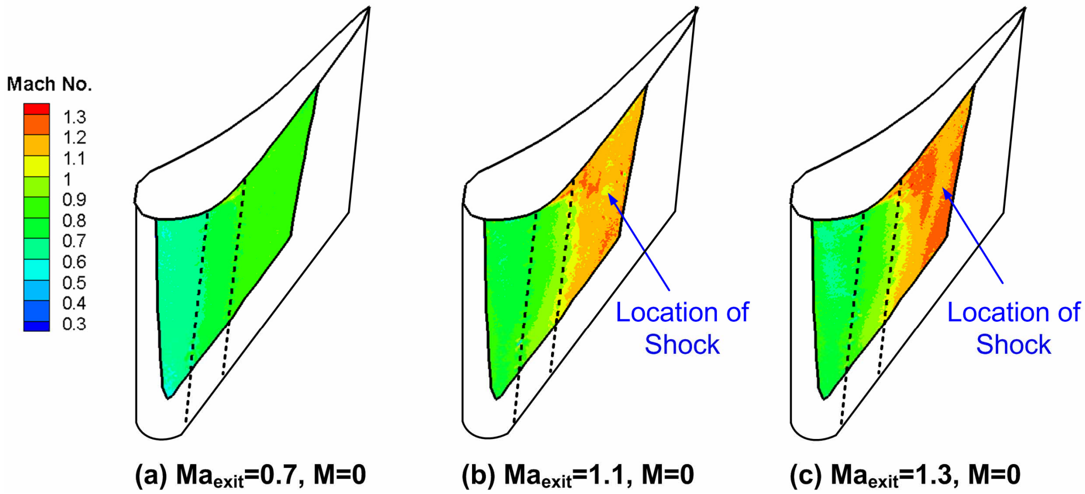

Fig. 4 Mach number distribution at different flow conditions (a) Ma$_{exit}$=0.7 (b) Ma$_{exit}$=1.1 (c) Ma$_{exit}$=1.3

EXPERIMENTAL SETUP

The test section consisted of a stationary blow-down facility with a 5-vane annular cascade with a removable test vane (**Fig. 1(a)**). A schematic of the optical setup is shown in **Fig. 1(b)**. Due to the safety concern while operating at high pressure, a limited size of window manufactured by stereolithography (SLA) process is used to view the interested area. Surface near the leading edge and trailing edge are out of visual range and can not be seen.

During the blow-down test, the cascade exit air velocities were set at exit Mach number (Ma$_{exit}$) 0.7, 1.1, and 1.3. The exit velocity was continuously monitored using a Pitot-static pressure probe placed downstream of the cascade. The blow-down facility could maintain steady flow in the cascade for about 1 minute. Compressed air stored in tanks entered a high flow digital control valve, which could maintain steady flow receiving downstream pressure feedback. The control valve could maintain a velocity within 2% of desired value. A grid was placed upstream of the cascade and generated turbulence level of 10% at test section inlet. The average length scale was approximately 1.5cm.

A scaled model of the Honeywell vane was placed in the center of annular cascade. Test vane manufactured by Selective Laser Sintering (SLS) process. **Figure 2(a)** shows the unique shape and cooling hole locations of the vane. It has a various height converges from leading to trailing edge. The leading edge of the test vane is equipped with three rows of showerhead film cooling holes; the middle row is aligned with the stagnation line. Three leading edge rows are staggered with respect to one another. Each showerhead row has 7 radial-angle cylindrical holes with a hole-to-hole spacing of s/d = 6.9. Two row of compound-angle shaped holes (SS1, SS2) on the suction side with a hole-to-hole spacing of s/d = 7.3. The shaped holes have a typical design of metering length and expansion angle in three directions. In **Fig. 2(a),** shaded area represents the actual portion from the view of the camera. Coolant is delivered from three straight passages as shown in **Fig. 2(b)**. Flow in each passage is individually controlled by a rotameter.

INSTRUMENTATION

To monitor the exit velocity, a Pitot-static probe is stationed 75% Cx distance downstream of the test vane. Before applying PSP to the test blade, it is coated with black paint. The black paint acts as a binder for PSP. The neighboring vanes and the passages are also sprayed black to eliminate any stray reflection. The vane is then sprayed with 6-8 coats of PSP (Uni-FIB UF470) using an air brush. A strobe light (PerkinElmer MVS-7000 Series) fitted with a narrow band-pass interference filter (optical wavelength=520nm) is used as the illumination source. The light is directed on to the vane surface by a flexible dual fiber-optic guide. Upon excitation, the PSP coated surface emits light of wavelength higher than 600nm. A 12-bit scientific grade CCD camera (Cooke Sensicam QE with CCD temperature maintained at 258K using 2-stage peltier cooler), fitted with a 35mm lens and a 600nm long-pass filter, records the intensity. The filter mounted on the camera is chosen such that no reflected light from the illumination source is able to pass through. The resolution obtained from the camera is 0.1mm/pixel.

The camera and the strobe light are triggered simultaneously using a 10 Hz pulsed TTL signal from a function generator. A total of 100 TIF images are captured and ensemble-averaged to get the emission intensity. In-house computer programs convert intensity into pressure and then to film-cooling effectiveness.

PRESSURE SENSITIVE PAINT

Measurement Theory

To obtain surface pressure data, pressure sensitive paint (PSP) technique is used. A basic PSP system is shown in **Fig. 3(a)**. The test surface is sprayed with a layer of special paint. The paint is composed of photo-luminescent molecules and an

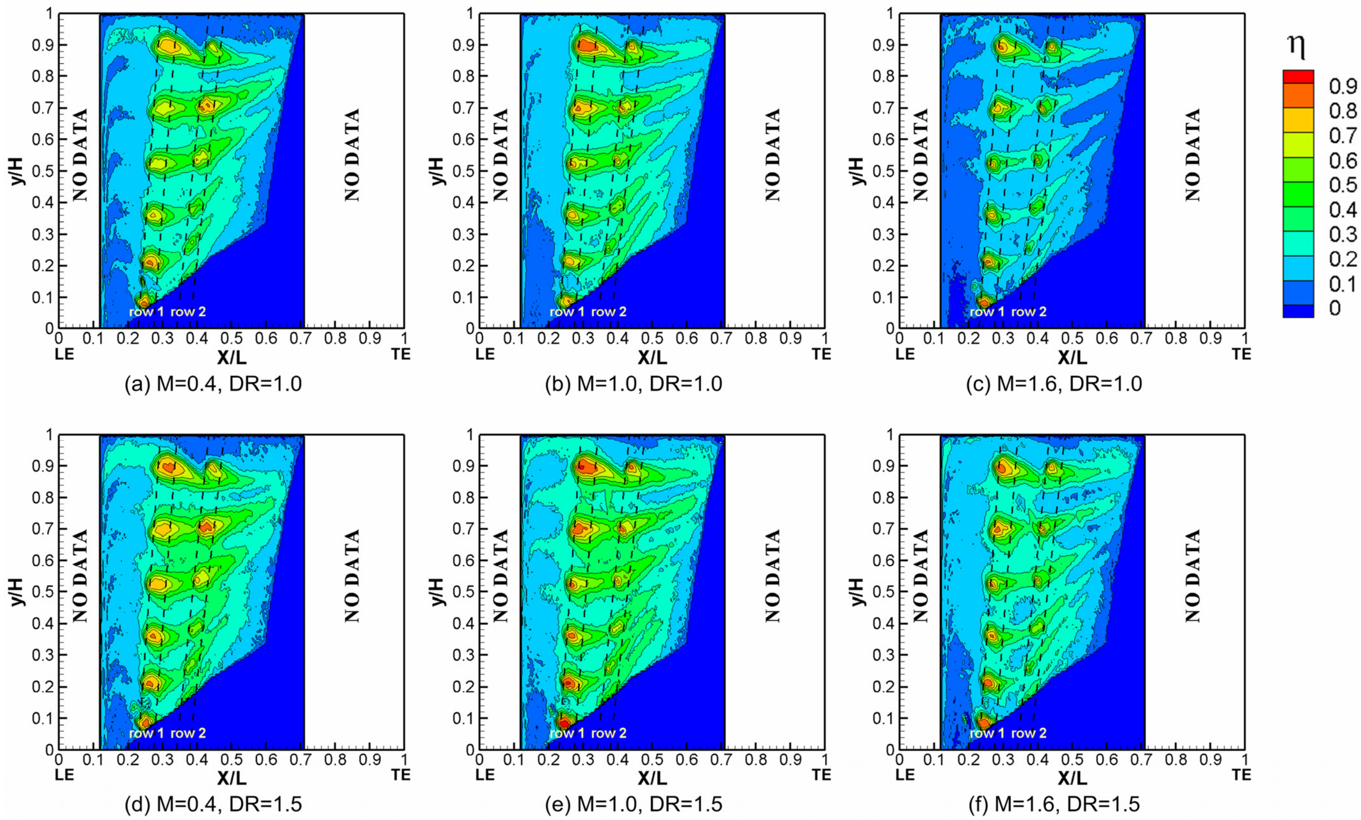

Fig. 5 Effect of blowing ratio and density ratio on adiabatic effectiveness at Ma_{exit}=0.7

oxygen-permeable polymer binder, both dissolved in a solvent. When excited by a light in the green region of the spectrum (around 520 nm and a bandwidth of 20 nm), the paint emits light in the red region (>600nm). The excited electrons of the PSP emit photons in the red range of the spectrum to fall back to their degenerate state. Another radiation-free path to the degeneration state is due to interaction with oxygen molecules. This is known as oxygen quenching. The intensity of the emitted light reduces with an increase in concentration (i.e. partial pressure) of oxygen adjacent to the PSP layer. Further details on the use of PSP for pressure measurements can be obtained from McLachlan and Bell [24].

Calibration of PSP

The emitted light is recorded by a scientific grade CCD camera equipped with a red-filter (to ensure none of the exciting green light is captured). The intensity of the emitted light (after correction for the background noise) is related to the partial pressure of oxygen surrounding the painted surface and is written as:

$$\frac{I_{ref} - I_{blk}}{I - I_{blk}} = f\left(\frac{\left(P_{O_2}\right)}{\left(P_{O_2}\right)_{ref}}\right) = K_1\left(P_{ratio}\right) + K_2\left(P_{ratio}\right) + K_3\left(P_{ratio}\right) \quad (1)$$

Here, I_{ref} is 'reference' intensity, typically corresponding with images acquired at atmospheric conditions. The corresponding (atmospheric pressure) is given by P_{ref}, and the atmospheric oxygen partial pressure is given by $P_{O2,ref}$. I_{blk} is the 'black' intensity, the back ground noise of the CCD camera, which corresponds with images acquired in a dark room. I corresponds with intensities acquired during the calibration. K_1, K_2, and K_3 are constants.

For calibration, a small block of copper with thin foil heater attached on one side and 7-8 coats of PSP on the other is placed inside a tightly sealed chamber having an optically clear window at the top, **Fig 3(b)**. Two T-type thermocouples are mounted on the PSP coated side to record the temperature. Calibration is performed at several pressures ranging between 0 and 2.0 atm covering the range expected during the experiments. At each pressure, emission intensity is recorded and a relationship between intensity and pressure is established.

The emitted light intensity by the pressure sensitive paint depends on both, the partial pressure of oxygen as well as the temperature of the surface. If this temperature dependency is not addressed properly during the analysis, temperature induced PSP errors could lead to inaccurate pressure data. **Figure 3(c)** shows the relationship between intensity and pressure at three different temperatures. I_{ref} in the numerator is common for all three curves and denotes the intensity obtained at 2 times of ambient pressure (2.0 atm) and temperature

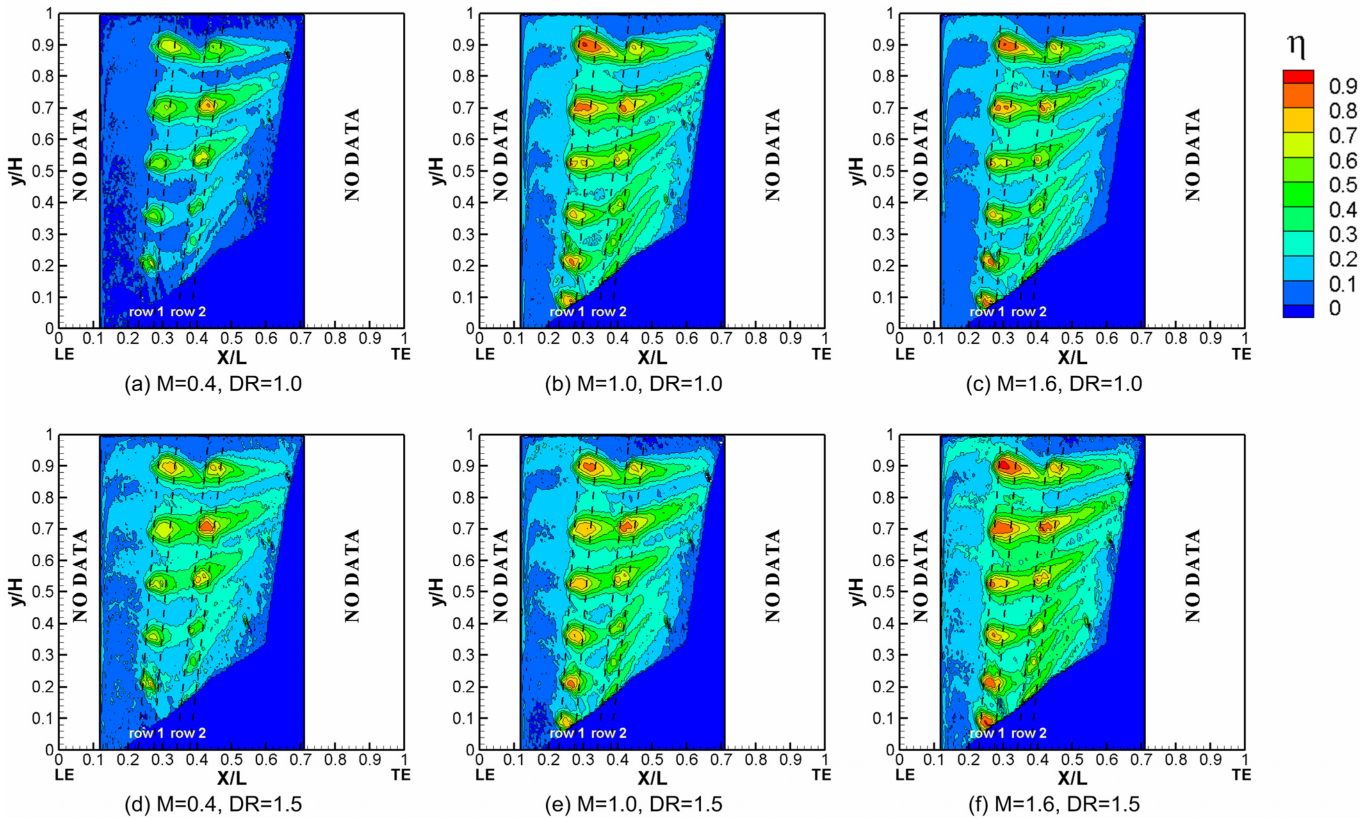

(a) M=0.4, DR=1.0 (b) M=1.0, DR=1.0 (c) M=1.6, DR=1.0
(d) M=0.4, DR=1.5 (e) M=1.0, DR=1.5 (f) M=1.6, DR=1.5

Fig. 6 Effect of blowing ratio and density ratio on adiabatic effectiveness at Ma_{exit}=1.1

(295K). It is found that if intensity, I_{ref}, is taken at tested pressure but at the corresponding heated temperature (295K/313K/334K), all the curves collapse into one as shown in **Fig. 3(d)**.

Film Cooling Effectiveness Calculation

To obtain film-cooling effectiveness, two different coolants are injected separately. Air (same as the mainstream) is used as one coolant and an oxygen-free foreign gas makes up the other coolant. The foreign gas mixes with or displaces air molecules on the PSP coated surface leading to a change in the emitted light intensity from the paint. By noting the difference in emitted intensity (and therefore partial pressure of oxygen) between the air and foreign gas injection cases, film-cooling effectiveness can be determined.

Using the heat and mass transfer analogy, based on works by Nicoll and Whitelaw [23] and Jones [25], the film cooling effectiveness can be expressed as a ratio of oxygen concentrations measured by PSP and is calculated using the following equation.

$$\eta = 1 - \frac{1}{\left\{\left(\frac{P_{O_2,air}}{P_{O_2,mix}} - 1\right)\frac{W_{fg}}{W_{air}} + 1\right\}} \quad (2)$$

In the above equation, $P_{O2,air}$ and $P_{O2,mix}$ correspond with pressure calculated from the intensity fields measured by two different injected coolants. The expression (**Eq. 2**) was originally derived by Charbonnier et al. [26], and has been used by Narzary et al. [27] and Rallabandi et al. [28]. In the special case where the molecular weight of the foreign gas is similar to that of air (e.g. nitrogen injection), the above equation can be simplified to:

$$\eta = 1 - \frac{P_{O_2,mix}}{P_{O_2,air}} \quad (3)$$

TEST CONDITIONS

A total of 30 sets of experiments are performed to study the effects of exit Mach number (Ma_{exit}), blowing ratio (M) and density ratio (DR) on vane suction side effectiveness. Five average blowing ratios – 0.4, 0.7, 1.0, 1.2, and 1.6 are selected for the tests. Leading edge showerhead holes were operated at the same blowing ratio as the suction side holes. Summary of experimental conditions are shown below:

(2)

Ma_{exit}=0.7 , DR=1.0 , M=0.4, 0.7, 1.0, 1.2, 1.6
Ma_{exit}=0.7 , DR=1.5 , M=0.4, 0.7, 1.0, 1.2, 1.6
Ma_{exit}=1.1 , DR=1.0 , M=0.4, 0.7, 1.0, 1.2, 1.6
Ma_{exit}=1.1 , DR=1.5 , M=0.4, 0.7, 1.0, 1.2, 1.6
Ma_{exit}=1.3 , DR=1.0 , M=0.4, 0.7, 1.0, 1.2, 1.6
Ma_{exit}=1.3 , DR=1.5 , M=0.4, 0.7, 1.0, 1.2, 1.6

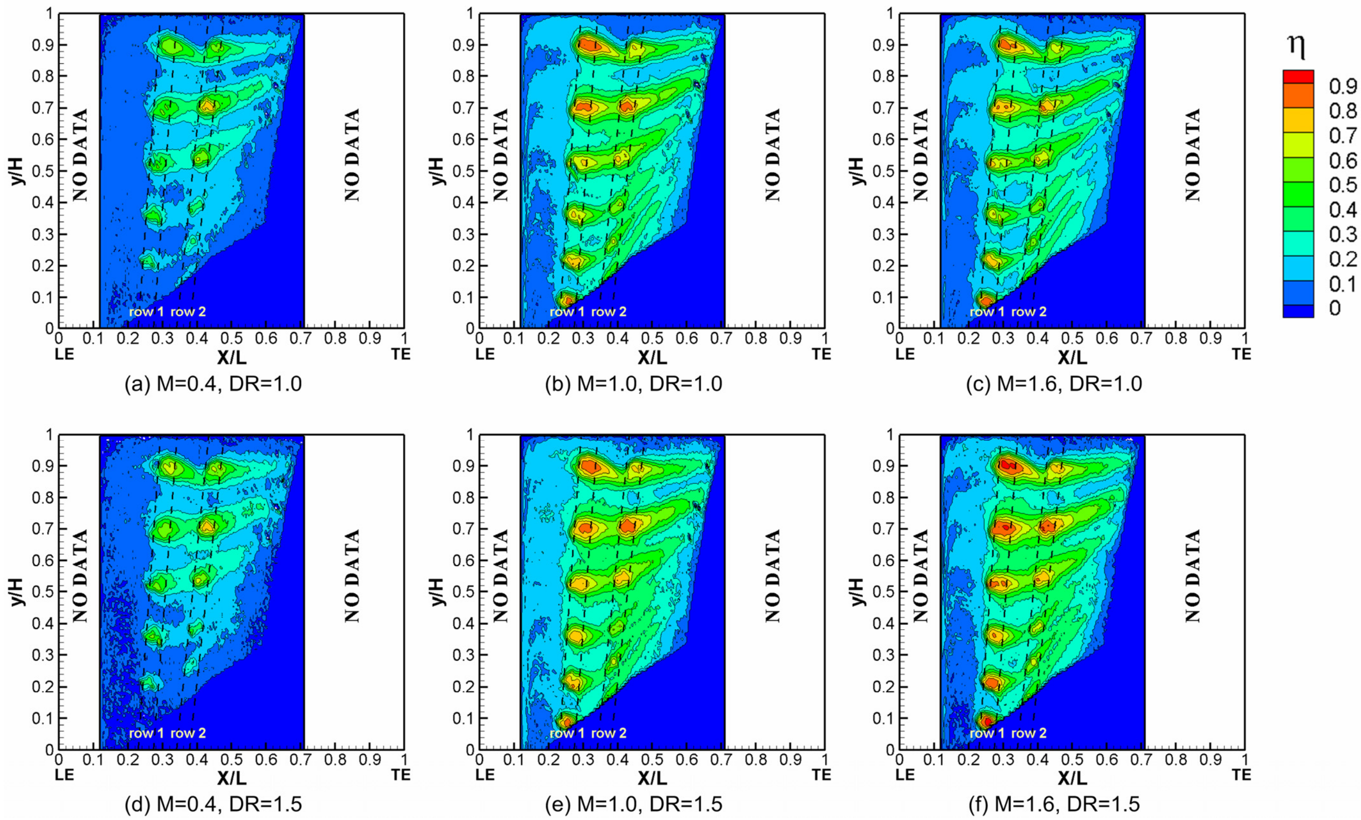

Fig. 7 Effect of blowing ratio and density ratio on adiabatic effectiveness at Ma_{exit}=1.3

The coolant supplied to the passages corresponding to each blowing ratio is calculated using the equation:

$$\dot{m}_c = \sum_{r=1}^{n} \left(M\right)\left(m''_m\right)_r \left(A_c\right)_r \tag{4}$$

where $\dot{m}_c$ is the average mass flow rate of coolant, M is the average blowing ratio, r refers to hole row, n is the number of rows around the cavity, m''_m is the mainstream mass flux over row r, and A_c is the total area of all coolant holes in row r. The mainstream mass flux ($\rho_m V_m$) over a particular row is determined from the local pressure information obtained by PSP. For examining density ratio (DR) effect, two foreign gases– industrial grade N_2, and industrial grade CO_2 serves as oxygen-free coolants in the PSP tests. The respective molecular weights are 1.0 and 1.5 times that of mainstream air.

Vane suction side Mach number is calculated by the local static pressure (measured by PSP) and inlet total pressure (measured by Pitot-static probe). **Figure 4** shows Mach number distribution at three exit Mach numbers, the discontinuous Mach number area has been pointed as shock region (e.g., in **Fig. 4(c)**, Mach number drops from 1.25 to 1.1, and then increase to 1.27). Film cooling rows are highlighted by dashed lines. The locations of the shock qualitatively agree with Sonoda et al. [18] and de la Loma et al. [19].

EXPERIMENTAL UNCERTAINTY

Uncertainties have been estimated based on the procedure described in Kline and McClintock [29] and Coleman and Steele [30]. The mainstream velocity is kept constant within ±2%. Uncertainty in setting the blowing ratio is ±3%. Based on an accuracy of ±1K for the thermocouple measurement and an accuracy of ±3% for PSP calibration, the uncertainty in adiabatic effectiveness amounts to ±2% for η=0.3 and ±8% for η=0.05.

EXPERIMENTAL RESULTS AND DISCUSSION

Adiabatic Film-Cooling Effectiveness

As mentioned earlier, due to the limited viewing window, the camera covers roughly 60% of the vane surface on the suction side. The abscissa and the ordinate of effectiveness contour are normalized with actual surface length (X/L) and vane height (y/H), respectively. **Figure 5**, **6** and **7** show the effect of blowing ratio and density ratio on film cooling effectiveness. Effect of exit Mach number is shown in **Fig. 8**. **Figure 9** shows the spanwise-averaged effectiveness for the four blowing ratios. The averaged effectiveness data is plotted for dimensional distance, X/Ms – the downstream distance (X) divided by the blowing ratio (M) and equivalent slot width (s). **Figure 10** plots the variation spanwise-averaged film cooling effectiveness with momentum flux ratio at selected positions along the vane at three different exit Mach numbers. The non-uniformity of coolant trace from both suction side rows may

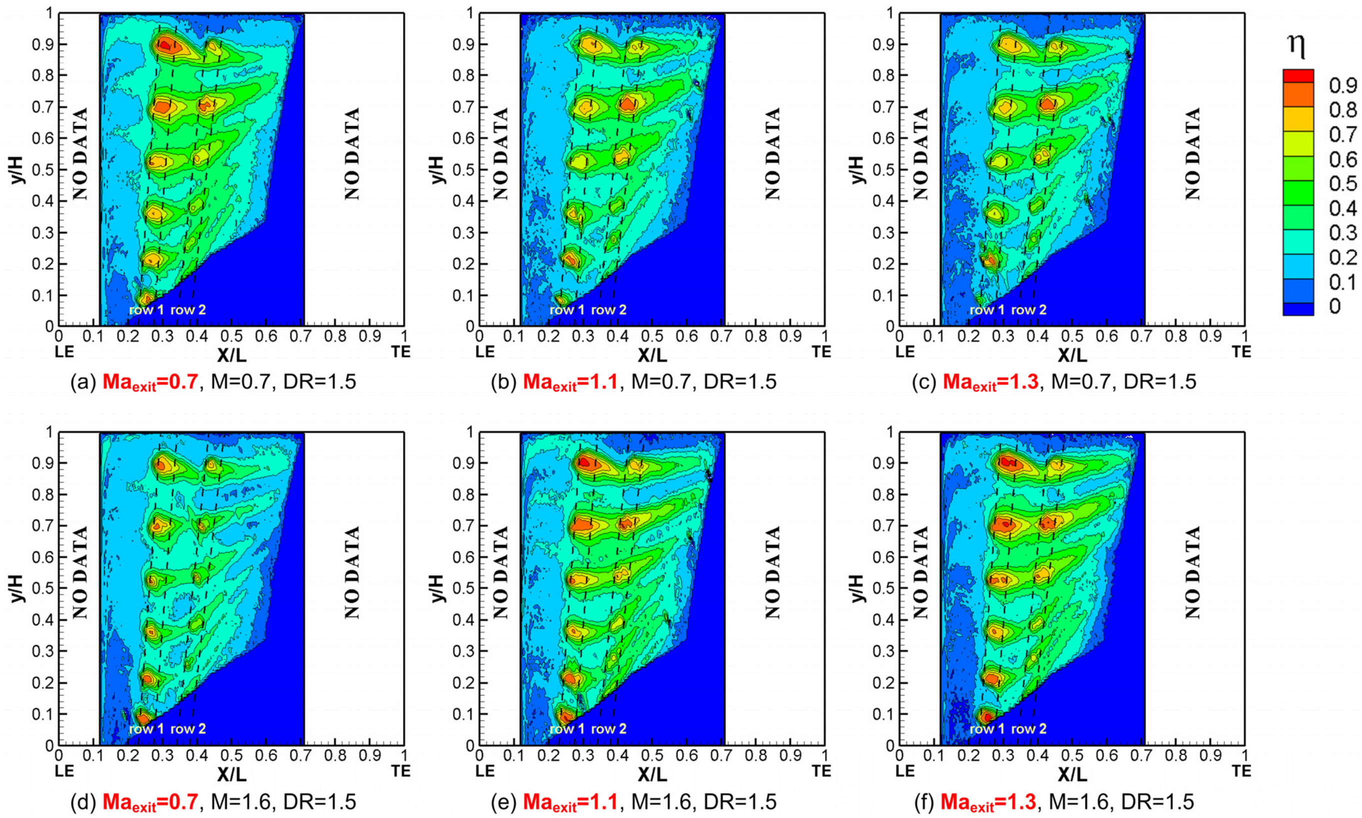

Fig. 8 Effect of exit Mach number on adiabatic effectiveness (DR=1.5, M=0.7, 1.6)

be attributed partly to the horseshoe vortex effect near the hub and tip; and partly to the coolant passage design that aids coolant stagnation at the top thereby allowing more coolant to discharge from the upper half of the passage. Effectiveness shown upstream of suction side rows are due to coolants carry over from the leading edge rows. With radial angle effect, more coolants are cumulated at upper portion.

Effects of blowing ratio and density ratio

Figure 5, **6** and **7** show the effect of coolant blowing ratio and density ratio on the contours of film cooling effectiveness at different flow conditions by injecting N_2 (upper half) and CO_2 (bottom half) as coolant. Three different blowing ratios are included, M=0.4 (left column), M=1.0 (middle column), and M=1.6 (right column).

At subsonic condition (Ma_{exit}=0.7), DR=1.0 case shows film cooling jets adhere to the vane surface at the lowest blowing of 0.4. On increasing the blowing ratio to 1.6, the coolant traces become shorter and reduce the thickness. It is an evidence of cooling jets tends to lift-off. Similar trend is observed at DR=1.5. The overall film cooling performance of DR=1.5 is better than that of DR=1.0. For a given blowing ratio, increasing the density ratio reduces the velocity of the coolant required to obtain the same blowing ratio, and therefore reduces the momentum of the coolant. Lower coolant momentum is less susceptible to "lift-off" than higher momentum coolant; as a result, when density ratio is increased from 1.0 to 1.5, there is a visible increase in effectiveness, both in terms of the trace length and the trace width.

In transonic flow (Ma_{exit}=1.1 and Ma_{exit}=1.3), as shown in **Fig. 6** and **7**, lowest cooling effectiveness occurs at the highest blowing ratio (M=1.6) for N_2. By injecting CO_2 as coolant, however, there is a different trend. No sign of lift-off in the range investigated can be attributed to the enhanced pressure caused by shock wave, which reduces the dissipation of coolant and makes the coolant jets deflect toward the vane surface. Larger blowing ratio indicates greater amount of supplied coolant, thereby film cooling effectiveness increases with blowing ratio. Present study has unique geometry design. It is therefore difficult to provide a complete comparison of past and present data. However, results are qualitatively similar to Ligrani et al. [15], and Kodzwa and Eaton [17] that denser coolant performs better, typically at higher blowing ratio in transonic flow. Spanwise-averaged effectiveness is plotted in **Fig. 9** for M=0.7, 1.0, 1.2, and 1.6. Lighter coolant is represented with solid lines; denser coolant ejection is indicated by dashed lines.

Effects of exit Mach number

Adiabatic film-cooling effectiveness distributions are shown in **Fig. 8** at Ma_{exit}=0.7 (left column), Ma_{exit}=1.1 (middle column), and Ma_{exit}=1.3 (right column). Each exit Mach number case corresponds with two blowing ratios, M=0.7 (upper half) and M=1.6 (bottom half). The coolant used is

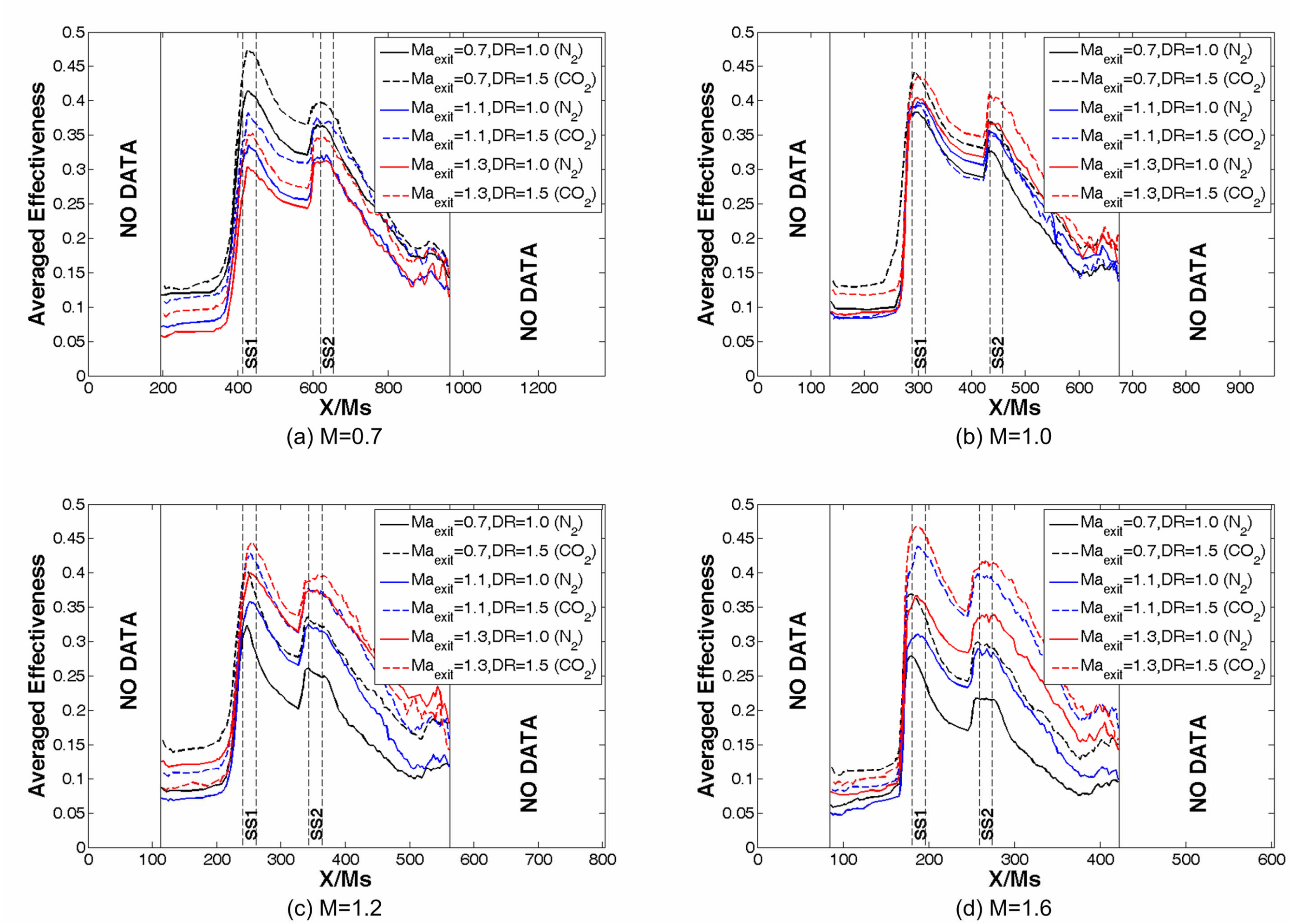

Fig. 9 Spanwise-averaged effectiveness as a function of exit Mach number and density ratio

CO_2, yielding a density ratio of 1.5. Results show that even the film holes on the suction side are all upstream of the passage throat where the shock exists, the presence of the shock downstream of the film hole can impact the film cooling effectiveness. At lower blowing ratio, film cooling effectiveness decreases with increasing exit Mach number, indicative of the coolant jet is affected by the present of shock, creates more mixing with mainstream air and results in lower effectiveness. However, as blowing ratio increases, effect of increasing exit Mach number is to increase effectiveness. This phenomenon can be postulated that the rapid rise in pressure caused by shock deflecting the coolant jet toward the vane surface at higher blowing ratio; as a result, it benefits film-cooling. Similar trend can be observed by comparing spanwise-averaged effectiveness of three flow conditions, as shown in **Fig. 9**. Flow conditions are specified by different colors, Ma_{exit}=0.7 (black), Ma_{exit}=1.1 (blue), Ma_{exit}=1.3 (red). Both the contour and the line plots report similar qualitative behavior.

<u>Effects of momentum ratio</u>

The combination effect of blowing ratio and density ratio is understood to be governed by the ratio of coolant momentum flux to the mainstream momentum flux. The momentum flux ratio (I) is defined thus:

$$I = \frac{\rho_c V_c^2}{\rho_m V_m^2} = \frac{\left(\rho_c V_c\right)^2 / \rho_c}{\left(\rho_m V_m\right)^2 / \rho_m} = \frac{M^2}{DR} \qquad (5)$$

The four locations in consideration are shown in **Fig. 10**. Position 1 is located on the SS1 row of the holes. Position 2 is located between the SS1 and SS2 holes. Position 3 is located on the SS2 row of the holes. Position 4 is situated downstream of the SS2 row of holes. **Figure 10** illustrates that the film cooling effectiveness is appropriately scaled by the momentum flux ratio, where the maximum film cooling effectiveness occurs at the optimum momentum flux ratio. The current study shows at any given momentum flux ratio, an increasing effectiveness trend with increasing density ratio. This can be attributed to the higher mass flow rate of higher density coolant. Similar trend was observed by Goldstein et al. [14], Ito et al. [11], and Sinha et al. [12]. Result also shows

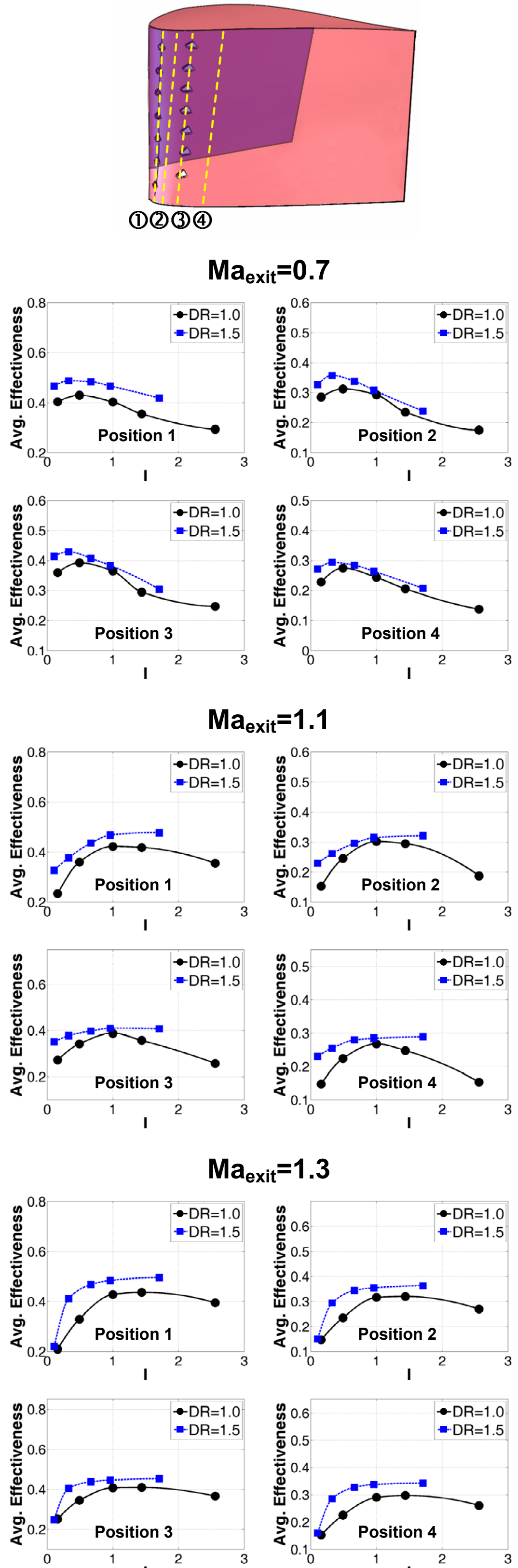

Fig. 10 Spanwise-averaged effectiveness as a function of momentum flux ratio

that at subsonic condition (Ma_{exit}=0.7), the optimum momentum flux ratio ($I_{optimum}$) decreases with density ratio. At the same blowing ratio, denser coolant results in a smaller momentum flux ratio. However, the trend is reversed in transonic flow (Ma_{exit}=1.1 and Ma_{exit}=1.3). Effectiveness values of denser coolant plateau over a wide range of momentum flux ratio, indicative of coolant jets still attached to the vane surface. The effect of increasing coolant density is to shift the peak effectiveness to greater momentum flux ratio, suggesting that coolant's mixing or lift-off behavior is delayed if shock wave takes place as opposed to subsonic flow field.

CONCLUSIONS

The present study uses PSP technique to measure adiabatic film-cooling effectiveness on the suction side of a transonic turbine vane. The effects of exit Mach number, coolant blowing, and coolant density are examined at different flow conditions, from subsonic to transonic. A modified equation (**Eq. 2**) is used to calculate the film-cooling effectiveness when foreign gas used is heavier than air (e.g. CO_2). The key highlights are presented below:

1) PSP method produces well defined coolant trace on the vane suction side surface even with heavier foreign gases at transonic condition.
2) When the flow becomes transonic, the rapid rise in pressure caused by shock eases the coolant jet to mix with mainstream and benefits film cooling effectiveness
3) At low blowing ratio, film cooling effectiveness decreases with increasing exit Mach number. The trend is reversed at high blowing ratio.
4) A coolant with higher density resists film cooling jet lift-off, resulting in a higher film cooling effectiveness.
5) At subsonic condition, $I_{optimum}$ decreases with density ratio. In the transonic flow, denser coolant obtains greater $I_{optimum}$ and peak effectiveness values plateau over a wide range of momentum flux ratio.

ACKNOWLEDGEMENT

The authors are grateful to Honeywell Engines, Turbine Department for their funding and support of this project.

REFERENCE

[1] Han, J. C., Dutta, S., and Ekkad, S. V., 2001, *Gas Turbine Heat Transfer and Cooling Technology*, Taylor & Francis, New York, 2001, Chapter 3.

[2] Goldstein, R. J., 1971, ''Film Cooling,'' *Advances in Heat Transfer*, Academic Press, San Diego, Vol. 7, pp. 321-379.

[3] Bunker, R. S., 2005 "A Review of Shaped Hole Turbine Film-Cooling Technology," *Journal of Heat Transfer*, Vol.127, n4, pp. 441-453.

[4] Bogard, D. G.., and Thole, K. A., 2006, ''Gas Turbine Film Cooling,'' *Journal of Propulsion and Power*, Vol.

22, n2, pp. 249-270.

[5] Han, J. C., and Rallabandi, A. P., 2010, ‘‘Turbine Blade Film Cooling Using PSP Technique,’’ *Frontiers in Heat and Mass Transfer*, Vol. 1, n1, pp. 1-21.

[6] Ligrani, P. M., Wigle, J. M., and Jackson, S. M., 1994b, ‘‘Film-Cooling From Holes With Compound Angle Orientations: Part 2 – Results Downstream of a Single Row of Holes With 6d Spanwise Spacing,’’ *Journal of Heat Transfer,* Vol. 116, n2, pp. 353-362.

[7] Schmidt, D. L., Sen, B., and Bogard, D. G., 1994, ‘‘Film Cooling with Compound Angle Holes: Adiabatic Effectiveness,’’ ASME Paper No. 94-GT-312.

[8] Ekkad, S., Zapata, D., and Han, J. C., 1997, ‘‘Film Effectiveness Over a Flat Surface With Air and CO_2 Injection Through Compound Angle Holes Using a Transient Liquid Crystal Image Method,’’ *Journal of Turbomachinery,* Vol. 119, pp. 587.

[9] Wright, L. M., Gao, Z., Varvel, T. A., and Han, J. C., 2005, ‘‘Assessment of Steady State PSP, TSP, and IR Measurement Techniques for Leading Edge Film Cooling,’’ *Proceedings of the ASME Summer Heat Transfer Conference.*

[10] Goldstein, R. J., and Jin, P., 2001, “Film Cooling Downstream of a Row of Discrete Holes With Compound Angle,” *Journal of Turbomachinery,* Vol. 123, pp. 222-230.

[11] Ito, S., Goldstein, R. J., Eckert, E. R. G.., 1978, ‘‘Film Cooling of a Gas Turbine Blade,’’ *Journal of Engineering for Power,* Vol. 113, pp. 476-481.

[12] Sinha, A. K., Bogard, D. G., and Crawford, M. E., 1991, ‘‘Film Cooling Effectiveness Downstream of a Single Row of Holes with Variable Density Ratio, ’’ *Journal of Turbomachinery,* Vol. 119, pp. 587.

[13] Ethridge, M. I., Cutbirth, M. J., Bogard, D. G., 2001, ‘‘Scaling of Performance for Varying Density Ratio Coolants on an Airfoil With Strong Curvature and Pressure Gradient Effects, ’’ *Journal of Turbomachinery,* Vol. 123, pp. 231-237.

[14] Goldstein, R. J., Eckert, E. R. G., and Burggraf, F., 1974, ‘‘Effects of Hole Geometry and Density on Three- Dimensional Film Cooling,’’ *Int. J. Heat Mass Transfer*, Vol. 17, pp. 595-607.

[15] Ligrani, P. M., Saumweber, C., Schulz, A., and Wittig, S., 2001, “Shock Wave – Film Cooling Interactions in Transonic Flows,” *Journal of Turbomachinery,* Vol. 123, pp. 778-797.

[16] Furukawa, T. and, Ligrani, P. M., 2002, ‘‘Transonic Film Cooling Effectiveness from Shaped Holes on a Simulated Turbine Airfoil,’’ *Journal of Thermophysics and Heat Transfe*, Vol. 16, pp. 228-237.

[17] Kodzwa,. P. M., and Eaton, J. K., 2010, ‘‘Film Effectiveness Measurements on the Pressure Surface of a Transonic Airfoil,’’ *Journal of Propulsion and Power*, Vol. 26, n4, pp. 837-847.

[18] Sonoda, T., Arima, T., Olhofer, M., Sendhoff, B., Kost, F., and Giess, P. A., 2006, “A Study of Advanced Hig-Loaded Transonic Turbine Airfoil,” *Journal of Turbomachinery,* Vol. 128, pp. 650-657.

[19] de la Loma, A., Paniagua, G., and Verrastro, D., 2008, “Transonic Turbine Stage Heat Transfer Investigation in Presence of Strong Shocks,” *Journal of Turbomachinery,* July, 2008, Vol. 130, 031019.

[20] Mhetras, S., and Han, J. C., 2006 “Effect of Unsteady Wake on Full Coverage Film-Cooling Effectiveness for a Gas Turbine Blade,” AIAA Paper No. AIAA-2006-3404.

[21] Narzary, D. P., Gao, Z., Mhetras, S., and Han, J. C., 2007 “Effect of Unsteady Wake on Film-Cooling Effectiveness Distribution on a Gas Turbine Blade with Compound Shaped Holes,” ASME Paper No. GT2007-27070.

[22] Gao, Z., Narzary, D. P., Mhetras, S., and Han, J. C., 2008, “Full-Coverage Film Cooling for a Turbine Blade With Axial-Shaped Holes,” *Journal of Thermophysics and Heat Transfer*, Vol. 22, n1, pp. 50-61.

[23] Nicoll, W., and Whitelaw, J., 1967, “The Effectiveness of the Uniform Density, Two-Dimensional Wall Jet (Two-Dimensional Wall Jets Effectiveness Measurements and Calculation Procedure for Injection Conditions),” *Int. J. Heat Mass Transfer*, Vol. 20, pp. 623-639.

[24] McLachlan, B., and Bell, J., 1995, “Pressure-Sensitive Paint in Aerodynamic Testing,” *Exp. Therm. Fluid Sci.*, 10, pp. 470–485.

[25] Jones, T., 1998, “Theory for the Use of Foreign Gas in Simulating Film Cooling,” *Int. J. Heat Mass Transfer*, Vol. 20, pp. 349-354.

[26] Charbonnier, D., Ott, P., Jonsson, M., Cottier, F., and Kobke, T., 2009, “Experimental and Numerical Study of the Thermal Performance of a Film Cooled Turbine Platform,” ASME Paper No. GT2009-60306.

[27] Narzary, D. P., Liu, K., Rallabandi, A. P., and Han, J. C., 2010, “Influence of Coolant Density on Turbine Blade Film-Cooling Using Pressure Sensitive Paint Technique,” ASME Paper No. GT2010-22781.

[28] Rallabandi, A. P., Li, S. J., and Han, J. C., 2010, “Unsteady Wake and Coolant Density Effects on Turbine Blade Film Cooling Using PSP Technique,” ASME IHTC 14, Washington DC, USA, IHTC 14-22911, Washington, DC, United States.

[29] Kline, S., and McClintock, F., 1953, “Describing Uncertainties in Single-Sample Experiments,” *Mechanical Engineering,* Vol. 75, pp. 3-8.

[30] Coleman, H.W., and Steele, W. G.., *Experimentation and Uncertainty Analysis for Engineers*, John Wiley & Sons, New York, 1989, Chaps. 3, 4.

